

Article

Lighting-Induced Changes in Central and Peripheral Retinal Thickness and Shape after Short-Term Reading Tasks in Electronic Devices

Elvira Orduna-Hospital ^{1,2}, Francisco J. Ávila ¹, Guisela Fernández-Espinosa ² and Ana Sanchez-Cano ^{1,2,*}¹ Department of Applied Physics, University of Zaragoza, 50009 Zaragoza, Spain² Aragon Institute for Health Research (IIS Aragon), 50009 Zaragoza, Spain* Correspondence: anaisa@unizar.es

Abstract: Background: To assess retinal and optical changes associated with near vision reading for different lighting conditions in electronic screens. Methods: Twenty-four young healthy subjects participated in the study; an iPad and an Ebook were chosen as stimuli for 5 min of reading task with different lighting conditions. Central and peripheral retinal thicknesses in the macular ETDRS areas by optical coherence tomography were analyzed. Results: Significant differences were found between basal retinal thickness and retinal thickness after reading with iPad and high illumination, in the N6 ($p = 0.021$) and I6 ($p = 0.049$) areas, and low illumination (S3: $p = 0.008$, N3: $p = 0.018$, I3: $p = 0.021$, N6: $p = 0.018$ and I6: $p = 0.020$), being thinner after reading. The same trend was observed after reading with an Ebook and high lighting in the N3 ($p = 0.037$) and N6 ($p = 0.028$). For low lighting conditions, only retinal thinning was observed. After reading, retinal shape analysis revealed significant changes from computed basal eccentricity for high lighting conditions only. At the periphery, those differences in eccentricity values were statistically significant for both lighting conditions. Conclusions: Young people can recover visual quality after 5 min of reading tasks at different lighting levels on electronic devices, while peripheral retinal expansion remains altered, especially at low lighting levels.

Keywords: aberrometry; accommodation; ambient lighting conditions; electronic reading devices; retinal thickness; retinal shape



Citation: Orduna-Hospital, E.; Ávila, F.J.; Fernández-Espinosa, G.; Sanchez-Cano, A. Lighting-Induced Changes in Central and Peripheral Retinal Thickness and Shape after Short-Term Reading Tasks in Electronic Devices. *Photonics* **2022**, *9*, 990. <https://doi.org/10.3390/photonics9120990>

Received: 1 November 2022

Accepted: 14 December 2022

Published: 16 December 2022

Publisher's Note: MDPI stays neutral with regard to jurisdictional claims in published maps and institutional affiliations.



Copyright: © 2022 by the authors. Licensee MDPI, Basel, Switzerland. This article is an open access article distributed under the terms and conditions of the Creative Commons Attribution (CC BY) license (<https://creativecommons.org/licenses/by/4.0/>).

1. Introduction

The relationship between myopia and accommodation is multifactorial, and it has been described that increased accommodative effort required during near work has been suggested as a causal factor in the development of myopia [1]. It has been widely documented how anterior pole structures change with myopia [2], and the literature also presents different changes in the posterior pole; for example, during accommodation when the lens thickens, the choroid thinness changes significantly [3]. In this case, the posterior pole seems to play an important role in accommodative performance and myopia progression. Currently, the anatomic complexities of each of these structures have not yet been elucidated, although changes in the posterior segment, and specifically in the choroid during accommodation, could promote myopic shift in some eyes. During accommodation, posterior pole elongation occurs together with a decrease in choroidal equatorial circumference, and a small but significant thinning of the choroid has been observed at high accommodation demand, which is greatest in the temporal and inferotemporal parafoveal choroid and increases with increasing eccentricity from the fovea [4,5]. These transient posterior pole modifications, after relatively short-duration accommodation tasks, are present, but they should be evaluated in depth to determine the ability and time period of recovery to the basal status, not only on the choroid, but also at the retinal level. Indeed, it has been described that retinal neurons are more widely spaced among individuals with myopia than among those with emmetropia [6,7], so this fact could explain the expansion of the

posterior pole and the thinner retina found in myopic subjects using optical coherence tomography (OCT) [8–10]. These studies have reported that peripheral retinal thickness decreases with increasing severity of myopia. Many studies have reported that the retina in the parafoveal regions and peripheral retina becomes thinner as the severity of myopia increases [9,11]. The precise visualization of its individual layers with OCT [12] correlates with histopathologic studies that showed that both inner plexiform and nuclear layers and outer plexiform layer contribute the most to retinal thinning, suggesting that photoreceptors, bipolar/horizontal cells, amacrine cells, and ganglion cells all contribute to retinal thinning due to a decrease in area density [13].

Globally, accommodation is a change in eye power to a more myopic situation. During this process, optical behavior has been widely described; in particular, higher-order aberration (HOA) affects the visual quality of the eye to provide cues to regulate accommodation. In particular, it has been described how differences in magnitude and sign can be found between emmetropic and myopic eyes [1], although the unaccommodated eyes recover their previous status immediately. This redundant work performed by the eye continuously means daily repetitive variations in its structure, and the more accommodation is needed, the more myopic the eye momentarily becomes.

Additionally, there is growing evidence from both human and animal studies of refractive error presenting that ambient light exposure is an important environmental factor involved in the regulation of eye growth. Documented seasonal variations in eye growth and refractive error progression in childhood support a potential role for ambient light exposure in the control of human eye growth. Different rates of growth, depending on the season, have been described, with slower rates in summer months and faster rates in winter months [14–17]. More specifically, greater average daily light exposure results in less axial growth of the eye in childhood, and a low but statistically significant relationship between them has been described [18].

A key knowledge gap is whether the thickness of different areas of the retina is more strongly associated with its shape under different lighting conditions after five minutes of near work reading tasks. This short-term accommodative demand produces a momentary myopization of the eye that is avoided after finishing the work. In young adults with a normal accommodative system, visual recovery is instantaneous, but structural changes could be temporally modified, specifically at central and temporal retinal areas, because they are more involved in these visual requirements than the nasal zone. This study focused on identifying structural retinal behavior based on fixed accommodative demand and controlled light levels reaching the corneal plane. To our knowledge, this is a novel study that has not been performed previously, considering the changes that occur in optical aberrations and in the thickness and eccentricity of the central and peripheral retina.

2. Materials and Methods

2.1. Sample Description

This prospective study, including 48 eyes from 24 healthy subjects from 18 to 33 years, was approved by the Comité de Ética de la Investigación de la Comunidad de Aragón (CEICA), with reference PI21-074, and the conduct of the study adhered to the tenets of the Declaration of Helsinki. After an explanation of the nature and possible consequences of the study, written informed consent was obtained from all participants before examination. Written assent was also obtained from all of them on the day of examination.

All subjects were included, except those who met the exclusion criteria to participate in the study, which were having binocular problems, best corrected visual acuity (BCVA) lower than 0.8 (20/25 on the Snellen chart) in one of the two eyes, refractive error greater than -4.50 D of myopia, $+2.50$ D of hyperopia and 1.50 D of astigmatism, or suffering from some ophthalmic or systemic pathology that affected vision or having used electronic devices one hour before the measurements. They had to have axial lengths (AL) between 22–24 mm to participate in the study.

2.2. Devices Used, Layout and Lighting

An Ebook, e-ink reader (ink pad 3, Pocket book International SA, China) model PB740, with a screen of 1404×1872 pixels, and an 8th generation iPad (Apple Inc, Cupertino, CA, USA) Model A2270, with a screen of 2160×1620 pixels, were used for reading tasks. In both devices, a white background and black letters of visual acuity 0.8, calibrated for the 50 cm at which the reading was made (+2.00 D accommodative demand), were used. The controlled maximum luminance of the Ebook was 79.60 cd/m^2 , and that of the iPad was 484.01 cd/m^2 , while the minimum luminance of the Ebook was 0.14 cd/m^2 , and that of the iPad was 1.56 cd/m^2 . Both reading devices were placed inside a controlled lighting cabinet to ensure optimal, repetitive, and correct lighting reaching the corneal plane of each participant in this study. To measure the conditions of maximum and minimum illumination that occur in the reading plane and in the corneal plane in each case, a luminancimeter (Konica-Minolta, LS-160) and a calibrated (NIST traceability) spectroradiometer model (STN-BLK-C-SR, StellarNet, Inc., Tampa, FL, USA) were used. They were used for analyzing the spectral power distribution in irradiance mode ($\mu\text{W/cm}^2$) from 380 nm to 780 nm and connected to a computer.

Inside the cabinet, a luminaire with cool white LEDs (6670 K correlated color temperature) was used to achieve proper lighting levels, so 945.65 lx and 4.38 lx reached the reading surfaces at maximum and minimum lighting conditions, respectively; meanwhile, with these previous conditions, 216.82 lx and 1.32 lx were measured at the position where subjects would have their corneal plane during the reading tasks. In addition to the light provided by the cabinet according to maximum lighting conditions and turning on the electronic devices, reaching the corneal plane 264.15 lx was measured with the Ebook and 260.10 lx with the iPad. On the other hand, when the conditions of the cabinet were minimum illumination, as well as minimum luminance of the devices, 1.63 lx for the Ebook and 1.62 lx for the iPad were obtained at the same corneal plane, maintaining equivalent spectral irradiance data for every wavelength from 380 nm to 780 nm.

An IRX3 Shack-Hartmann device (Imagine Eyes, Orsay, France) was used to perform the aberrometric measurements under scotopic lighting conditions. This equipment has a near-infrared source (780 nm), which is imaged on the retina, and arrays of microlenses with associated sensors detect directional information of the wavefront of light generated from it. After blinking, measurements were taken focusing on the Purkinje images obtained by aligning the instrument axis with the eye's pupil (axial conjugation between the instrument lenslet array and the eye's pupillary plane). The manufacturer's software automatically calculates the aberrometric data fitting the measured wavefront of a 4 mm fixed pupil diameter immediately after ending each five-minute reading task described previously. The real wavefront was analyzed with respect to the ideal to obtain the error of each measured eye in terms of total root mean square (RMS Total), low-order RMS (RMS LOA), and high-order (RMS HOA).

The AL was measured with the optical biometry IOLMaster[®]500 from Carl Zeiss Meditec (Carl Zeiss Meditec, Oberkochen, Germany) as the mean of 5 measurements and expressed in mm.

Each individual eye was imaged twice using a 3D OCT-1000 (Topcon Corporation, Tokyo, Japan). First, the subject was asked to look into the internal central fixation target to image the central retina, and then the internal fixation was moved horizontally 15° right for the right eye (RE) and 15° left for the left eye (LE) to image the temporal peripheral retina (Figure 1). In both cases, the macular cube protocol was performed. It provides a circular macular map analysis, divided into nine sectorial thickness measurements in three concentric circles with diameters of 1, 3 (inner), and 6 (outer) mm, forming the 9 Early Treatment Diabetic Retinopathy Study (ETDRS) area grid. The central or subfoveal area (1 mm, C), the 3 mm parafoveal ring with four areas, temporal inner (T3), superior inner (S3), nasal inner (N3), inferior inner (I3), four other areas belonging to the 6 mm perifoveal ring, temporal outer (T6), superior outer (S6), nasal outer (N6), and inferior outer (I6), were used to study the total retinal thickness (Figure 1). Once the macular maps

were automatically segmented to obtain total retinal thickness from the internal limiting membrane (ILM) to Bruch's membrane (BM), the thicknesses were shown in every ETDRS area. The quality of the scans was checked, and poor-quality scans were rejected.

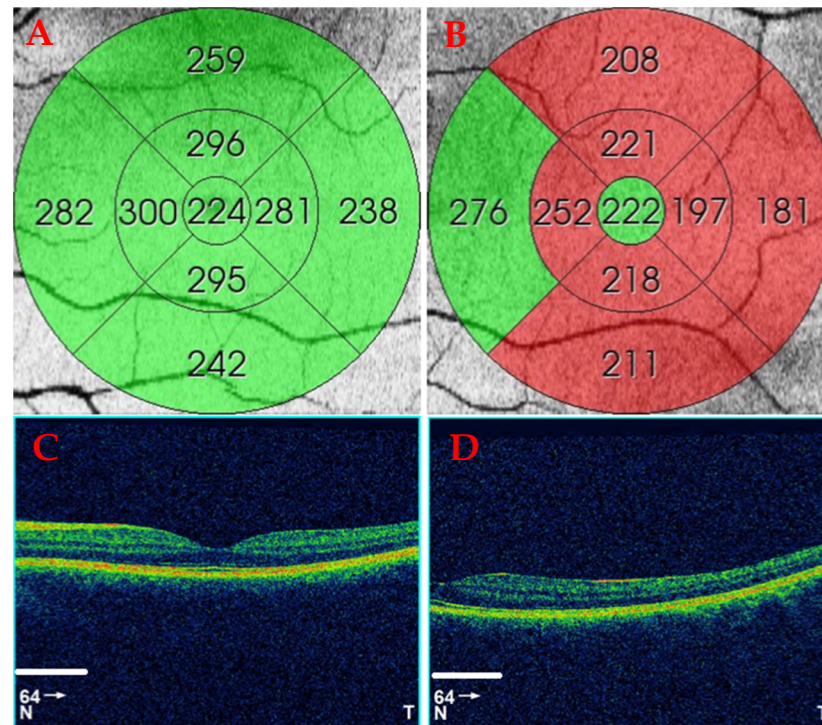


Figure 1. (Up) The 9 circular areas for a left eye. The 1 mm diameter central area (C), the 3 mm parafoveal ring with four areas: temporal inner (T3), superior inner (S3), nasal inner (N3) and inferior inner (I3). The 6 mm perifoveal ring: temporal outer (T6), superior outer (S6), nasal outer (N6), and inferior outer (I6). Optical coherence tomography (OCT) images for a left eye. The 9 ETDRS areas in the central retina (A) and the peripheral retina (B). Central retina B-scan (C) and peripheral temporal retina B-scan (D). Scale bars 1000 μm .

2.3. Experimental Protocol

The participants were asked not to use any type of electronic device one hour before taking the readings and not to perform close-up tasks so that it would not interfere with the baseline aberrometry and OCT measurements. The OCT images and aberrometry were always performed by the same observer between 4:00 p.m. and 7:00 p.m.

Aberrometry and central and peripheral OCT measurements were performed in scotopic conditions upon arrival of the participant and before starting any reading that would serve as baseline measurements. The participant stood with their chin and forehead resting on the chin rest 50 cm from the reading device (iPad or Ebook), with the text calibrated for a visual acuity of 0.8.

The subjects would take four readings of 5 min, each according to the four randomized assumptions to avoid bias in the measurements due to adaptation to light conditions: high ambient illuminance level (945.65 lx) with maximum iPad luminance (484.01 cd/m^2); high level of ambient illuminance (945.65 lx) with maximum luminance of the Ebook (79.60 cd/m^2); low ambient illuminance level (4.38 lx) with iPad minimum luminance (1.56 cd/m^2); and low level of ambient illuminance (4.38 lx) with minimum luminance of the Ebook (0.14 cd/m^2).

After each reading, an aberrometer measurement and both OCT images, one for the central retina and the other for the temporal peripheral retina, were taken again. There was a 15-min break between readings in which the subject was also unable to use electronic devices or perform close-up tasks.

2.4. OCT Image Segmentation Algorithm

A custom-written algorithm in MATLAB (R2020a, Mathworks, MA, USA) was applied to obtain retinal segmentation at the retinal pigment epithelium (RPE) layer and then obtain a conical fitting to compute the eccentricity values of the retinal shape in both central and peripheral locations as described in the previous subsection. Figure 2 shows a flux schematic diagram of the proposed algorithm proposed in this work. First, the program reads the input raw OCT image and converts it from RGB color to an 8-bit image (RGB to gray). Next, the program uses the Canny filter for automatic edge detection of the RPE. Figure 3 shows an example of RPE segmentation in two different OCT images.

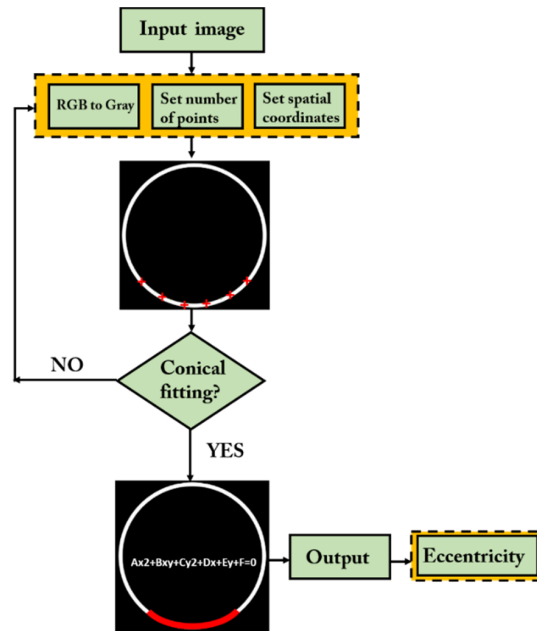


Figure 2. Schematic diagram of the proposed segmentation algorithm.

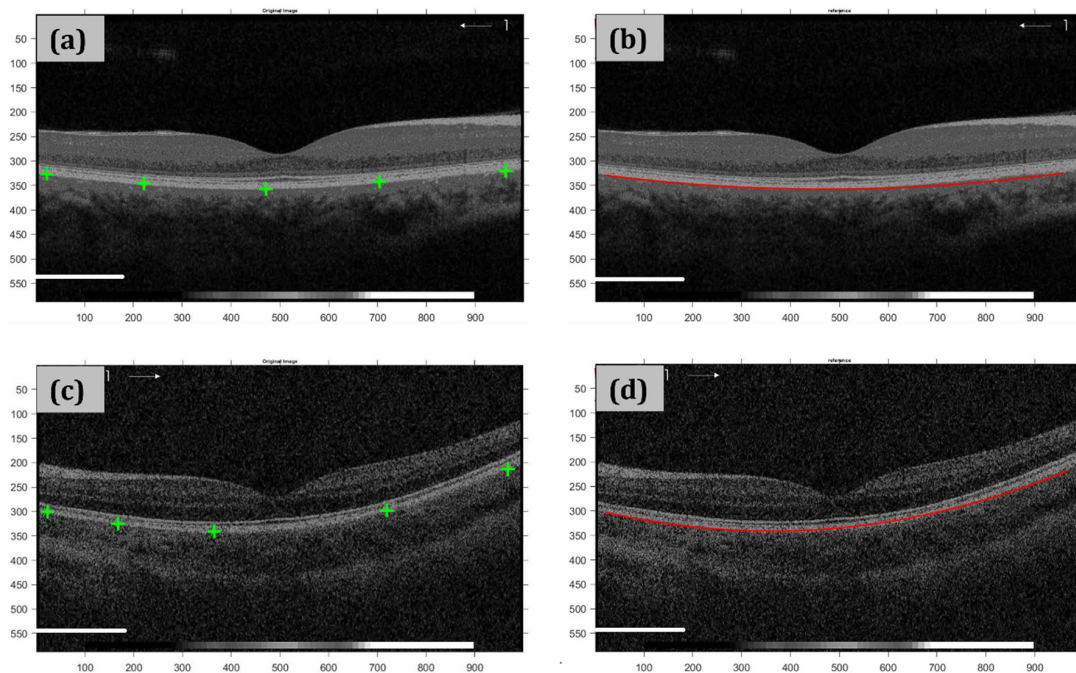


Figure 3. OCT Example of detection of RPE in two different OCT images (a,c) and final conical segmentation (b,d). Scale bars 1000 μm .

Once the length of the RPE through the entire image is known, the user selects the minimum number of points over the epithelium edge from which the spatial coordinates will be calculated. Once the coordinates are obtained, the program computes a conical fitting. If a conical equation can be obtained, the eccentricity is computed from its coefficients. Otherwise, the program asks the user to set a different number of points to obtain a new set of spatial coordinates.

2.5. Statistical Analysis

The measurements of the variables to be studied were recorded in an Excel database (Microsoft Office Excel 2011, Microsoft Corporation). Statistical analysis was performed using the Statistical Package for the Social Sciences (SPSS 20, SPSS Inc., IBM Corporation, Somers, NY, USA). Normal distribution of the values was studied with the Kolmogorov-Smirnov test. To compare retinal thicknesses and aberrometries under the different lighting conditions, the paired sample t-test and the Wilcoxon signed-rank test were used, respectively, since the retinal thicknesses have a normal distribution and the aberrometries did not. All retinal shape analysis was performed with MATLAB (R2020a, Mathworks, MA, USA). A *p* value < 0.05 was considered statistically significant.

3. Results

Twenty-four young healthy subjects participated in the study, of which 16 were men (66.66%) and eight were women (33.33%), with a mean age of 23.37 ± 3.59 years (range 18–33). A mean spherical equivalent refractive error of -0.75 ± 1.50 D (range -4.50 to $+2.50$) and a mean AL of 23.24 ± 0.73 mm (range 22 to 24) were obtained.

3.1. Aberrometric Measurements

Aberrometric data followed nonnormal distribution; therefore, nonparametric tests were used for statistical analysis between reference and after different lighting conditions (Table 1). Mean RMS \pm standard deviation (\pm SD) for total, LOA, and HOA (3rd order and 4th order) were evaluated to find no statistically significant differences.

Table 1. Aberrometry values; mean \pm standard deviation (\pm SD) in μ m. No statistical differences were found between measurements (*p* > 0.05).

	Previous	iPad_max		iPad_min		Ebook_max		Ebook_min	
	Mean \pm SD [min-max]	Mean \pm SD [min-max]	<i>p</i>	Mean \pm SD [min-max]	<i>p</i>	Mean \pm SD [min-max]	<i>p</i>	Mean \pm SD [min-max]	<i>p</i>
RMS	0.554 \pm 0.582	0.589 \pm 0.644	0.886	0.632 \pm 0.655	0.519	0.604 \pm 0.646	0.215	0.609 \pm 0.655	0.926
TOTAL	[0.089–2.661]	[0.125–2.580]		[0.124–2.627]		[0.136–2.696]		[0.105–2.554]	
RMS	0.529 \pm 0.591	0.566 \pm 0.653	0.876	0.610 \pm 0.663	0.405	0.579 \pm 0.656	0.211	0.588 \pm 0.663	0.943
LOA	[0.060–2.659]	[0.085–2.575]		[0.073–2.622]		[0.111–2.695]		[0.073–2.549]	
RMS	0.122 \pm 0.040	0.118 \pm 0.039	0.345	0.126 \pm 0.041	0.707	0.127 \pm 0.041	0.460	0.114 \pm 0.037	0.312
HOA	[0.065–0.234]	[0.073–0.238]		[0.076–0.257]		[0.079–0.271]		[0.059–0.215]	
RMS 3rd	0.084 \pm 0.032	0.088 \pm 0.039	0.807	0.093 \pm 0.037	0.242	0.096 \pm 0.043	0.053	0.082 \pm 0.038	0.468
ORDER	[0.035–0.186]	[0.0008–0.218]		[0.046–0.195]		[0.032–0.022]		[0.018–0.178]	
RMS 4th	0.049 \pm 0.025	0.044 \pm 0.020	0.613	0.053 \pm 0.027	0.778	0.049 \pm 0.021	0.615	0.047 \pm 0.019	0.154
ORDER	[0.018–0.123]	[0.012–0.146]		[0.016–0.139]		[0.011–0.108]		[0.019–0.088]	

3.2. Retinal Thickness and Volume

When comparing the OCT thickness measurements of the central basal retina with the retinal thickness values measured after reading with the iPad in the nine ETDRS areas, statistically significant differences were observed for both lighting conditions in the I6 area, being thicker after reading in both cases with respect to the basal measurement (221.24 ± 24.44 μ m basal thickness vs. 253.29 ± 15.37 μ m high lighting; *p* < 0.001, and , basal thickness vs. 249.65 ± 23.28 μ m low lighting; *p* < 0.001). There were no differences between minimum illumination and maximum illumination after reading with the iPad in the central retinal thickness (Figure 4).

iPad

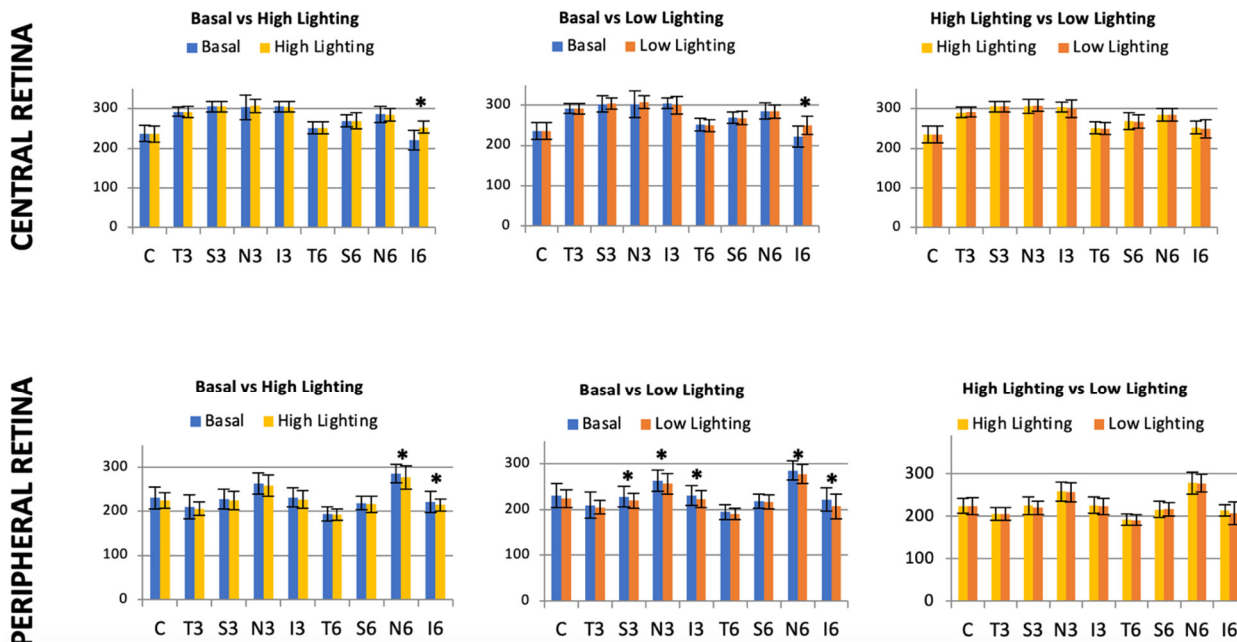


Figure 4. Mean and standard deviation (SD) of the central and peripheral retinal thicknesses (μm) in high and low lighting conditions in the nine ETDRS areas measured by 3D OCT-1000 after reading with an iPad device. Differences that reached statistical significance ($p < 0.05$) are marked with *.

Regarding the peripheral retina and iPad reading, significant differences were found between basal retinal thickness and retinal thickness after reading with high illumination in the N6 ($285.82 \pm 20.92 \mu\text{m}$ basal thickness vs. $276.69 \pm 26.72 \mu\text{m}$ high lighting; $p = 0.021$) and I6 ($221.24 \pm 24.44 \mu\text{m}$ basal thickness vs. $214.40 \pm 13.56 \mu\text{m}$ high lighting; $p = 0.049$) areas; in both cases, the retina was thinner after reading (Figure 4).

When comparing the basal peripheral retina after reading with the iPad in conditions of minimum illumination, there were statistically significant differences in five areas (S3: $p = 0.008$, N3: $p = 0.018$, I3: $p = 0.021$, N6: $p = 0.018$, and I6: $p = 0.020$); in all cases, the retina was thinner after reading (Figure 4). There were also no differences between minimum illumination and maximum illumination after reading with the iPad in the peripheral retinal thickness.

With Ebook reading, no differences were found in central retinal thickness between central basal measurements and either of the two lighting conditions or between minimum and maximum lighting. In contrast, statistically significant differences were found between basal peripheral retinal thickness and retinal thickness after reading with an Ebook and high lighting in the N3 ($263.85 \pm 23.65 \mu\text{m}$ basal thickness vs. $257.43 \pm 22.92 \mu\text{m}$ high lighting; $p = 0.037$) and the N6 ($285.72 \pm 20.53 \mu\text{m}$ basal thickness vs. $278.15 \pm 22.53 \mu\text{m}$ high lighting; $p = 0.028$) areas, which were thinner after reading in both cases. For low lighting conditions, only retinal thinning was observed in the N6 area ($284.74 \pm 21.00 \mu\text{m}$ basal thickness vs. $276.66 \pm 24.41 \mu\text{m}$ low lighting; $p = 0.037$). There were no differences in thickness when comparing the measurements after reading with both illuminations (Figure 5).

Ebook

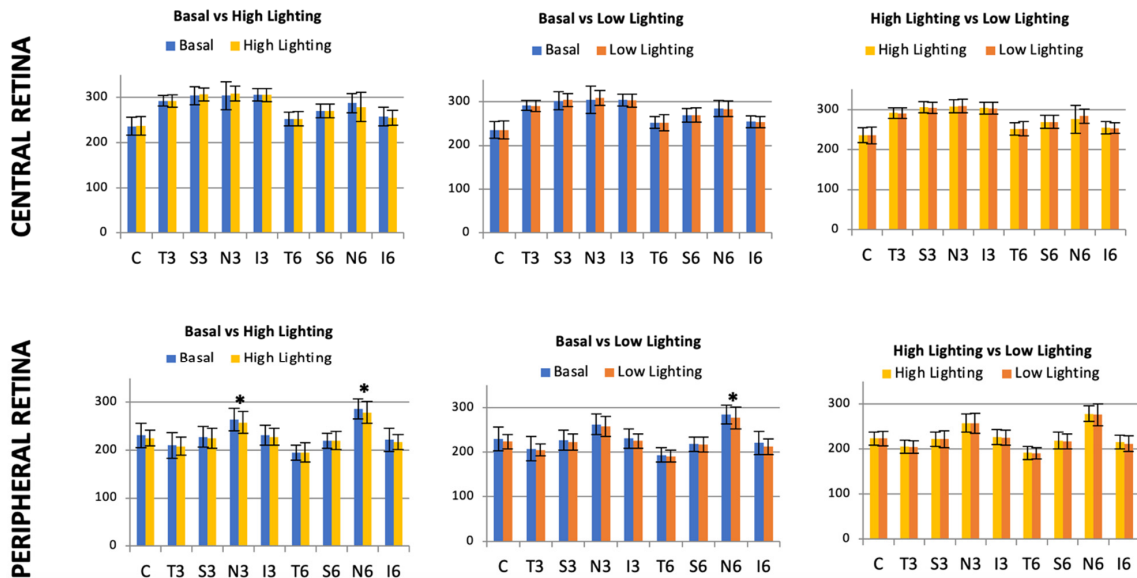


Figure 5. Mean and standard deviation (SD) of the central and peripheral retinal thicknesses (μm) in high and low lighting conditions in the nine ETDRS areas measured by 3D OCT-1000 after reading with an Ebook device. Differences that reached statistical significance ($p < 0.05$) are marked with *.

Regarding the total retinal volume, including the nine areas together, statistically significant differences were found only in the peripheral retinal volume between the basal thickness measurement and after reading with iPad in low light conditions ($6.52 \pm 0.52 \text{ mm}^3$ basal volume vs. $6.32 \pm 0.44 \text{ mm}^3$ low lighting volume; $p = 0.008$), with less volume after reading, and between the peripheral retinal volume and iPad reading between lighting conditions ($6.40 \pm 0.41 \text{ mm}^3$ high lighting volume vs. $6.32 \pm 0.44 \text{ mm}^3$ low lighting volume; $p = 0.023$) (Figure 6), being lower in low lighting conditions.

VOLUME

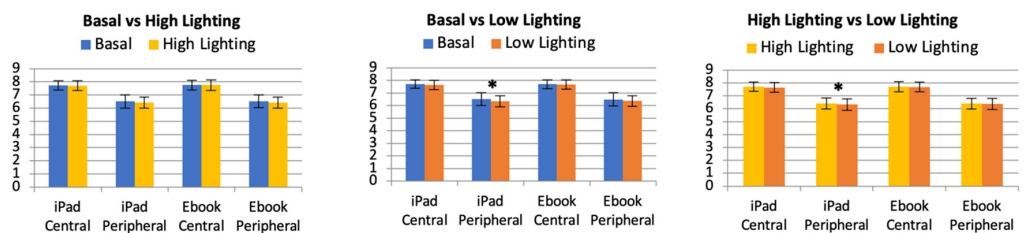


Figure 6. Mean and standard deviation (SD) of the central and peripheral retinal volume in high and low lighting conditions measured by 3D OCT-1000 after reading with both devices (iPad and Ebook). Differences that reached statistical significance ($p < 0.05$) are marked with *.

3.3. Retinal Shape

The described OCT retinal segmentation algorithm was applied to the images in both central and peripheral retinal locations in different lighting conditions and after reading Ebook and iPad devices. The computed eccentricity values are shown in Figure 7. Regarding the central retina, retinal eccentricity was found to change to lower values after reading with iPad and Ebook devices in both high- and low-light conditions. Those changes in central retinal shape were found to be significantly lower after reading with iPad and Ebook devices in high lighting conditions only (with regard to those basal values).

However, no significant differences were found between the basal values and after reading the iPad and Ebook in low lighting conditions.

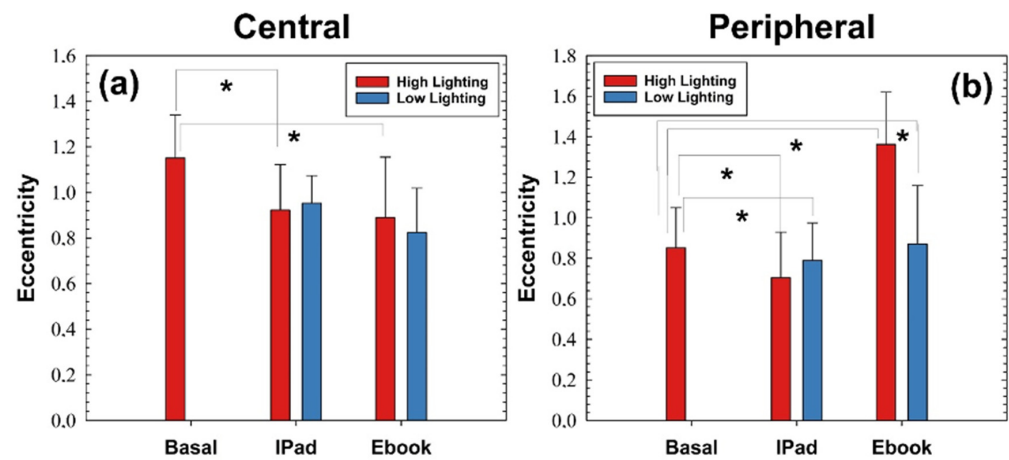


Figure 7. Mean and standard deviation (SD) of the central and peripheral retinal shape in high and low lighting conditions. Statistical differences ($p < 0.05$) are marked with asterisks (*).

At the periphery, eccentricity values revealed more retinal sensitivity to light conditions in terms of morphological adaptations. As shown in Figure 7b, significant retinal changes were found between basal conditions and those calculated after reading with the iPad and Ebook in both high- and low-light conditions. Whereas the peripheral retinal shape tended to be more elliptical after reading with the iPad, the Ebook device showed a significant increase in eccentricity values in high lighting conditions and no changes in low lighting conditions with regard to the basal values.

Figure 8 compares the impact on retinal shape in each reading device and retinal location in both lighting conditions (i.e., high versus low lighting conditions). No significant changes were found after changing the lighting conditions while reading with the iPad device in either the central or the peripheral retinal locations. However, the retinal eccentricity values were found to be significantly lower in both central and peripheral locations after reading with the Ebook device. That is, in high lighting conditions, the retinas exhibit a parabolic shape (Ebook device) that undergoes a morphological modification to a parabolic shape in both central and peripheral locations.

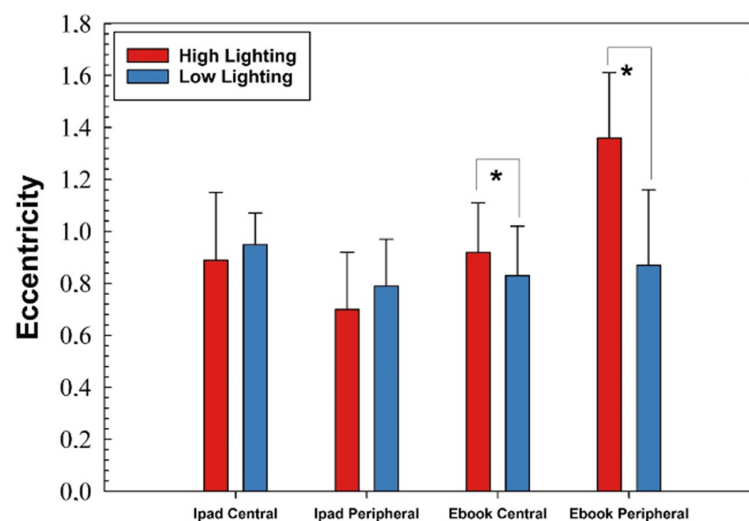


Figure 8. Mean and standard deviation (SD) of the eccentricity values for each read electronic device and retinal location as a function of the lighting conditions. Statistical differences ($p < 0.05$) are marked with asterisks (*).

4. Discussion

The current study investigated the influence of lighting on retinal shape and thickness in young adults after five minutes of accommodative stimuli. Before and after reading tasks with different lighting conditions, *in vivo* on-axis and off-axis retinal imaging was performed using OCT. Additionally, custom-made software was used for distortion correction of the central 9 mm arrangement of the foveal centered OCT scan to evaluate changes in retinal thickness and curvature, taking the RPE as a reference. On-axis aberrometry was performed before and after these reading tasks to ensure that eyes recovered their visual reference state and, therefore, structural changes were analyzed without visual dependence. The performed statistical analysis could be of greater correlation between the two eyes of an individual compared with the correlation between two individuals, since both eyes were under the same ambient light conditions, found results remain valid and consistent [19,20].

Although there are large differences in the findings from diverse studies, it remains an open question about how lighting can influence the shape of the retina and, consequently, diseases such as the progression of myopia related to near tasks and low lighting levels [21]. There is evidence that choroidal thickness is highly dependent on ametropia, with reduced choroidal thickness in less hypermetropic eyes [1]; during accommodation, the eyes momentarily become more myopic, so the findings in this study can offer a new viewpoint to understand this question. First, electronic devices in general are considered to be a potential cause of myopia progression due to the maintained accommodative demand produced by their use [22]. The absence of aberrometric differences between the baseline and the posterior reading with both e-ink and iPad suggests that, concerning the accommodative stimuli, both are indeed very similar after short-term near visual tasks. This implies that the ability of the lens to focus on the retina is highly influenced, at least, by the age of the subjects and their visual quality. In our study, all the subjects were under 33 years old and had both good accommodative quality and quantity. Meanwhile, we found, in each subject, different aberrometric profiles as baseline, and reading tasks changed them to be recovered as soon as the near tasks were concluded, irrespective of the device used or the light level. These results are supported by the 6 mm ETDRS central grid, in which the retinal thickness analysis had a similar behavior to the aberrometric results previously described.

As shown by this study, the peripheral retina seems to have a different behavior after finishing near tasks; its shape is modified by the reading requirements, and its recovery is not complete or is slower than that of the central retina. In particular, the more curved the retina, the thinner it is in a cross-section of 6 mm to 9 mm from the fovea to the temporal side, signifying a peripheral hyperopic defocus. In this study, both temporal curvature and thickness suffered combined modification, suggesting a delay in the recovery of the structural characteristics.

Regarding the spectral power distribution of the lighting, both luminance and spatial frequency content of the stimuli and axial blur on retina have all been demonstrated to be myopigenic cues when they are temporally maintained [23]. Meanwhile, our results show an instantaneous off-axis modification that, in this case with our custom-made software, has been evaluated on a unique section of the central retina. To avoid limitations in the study and to have a wider area, the ETDRS analysis performed with OCT showed important structural changes in both thickness and volume that cannot be omitted or attributed to the accommodation because both electronic devices are located at the same distance to the observer, producing the same +2.00 D accommodative stimuli.

During reading tasks, accommodation occurs, and anatomical changes are present to focus near stimuli on the retina. It has been previously reported that, in addition to dimensional changes in the anterior segment, during maximum accommodation in young adults, the retinal thickness was reduced, although in a 4 mm × 4 mm macular area centered at the fovea. In this sense, no significant quadrant-dependent difference in retinal volume change was found, which indicates that neither retinal stretching nor distortion was quadrant-dependent during accommodation [24]. Although this occurs, retinal modifications are supposed to be instantaneously correlated with accommodation

and disaccommodation, and found in the central retina, but our results show peripheral modifications that could be a consequence of light because all stimuli demand the same accommodation, in this case +2.00 D.

Choroid plays a potential role in eye growth regulation. Changes in choroidal thickness accompany eye growth, being more marked in highly myopic eyes, leading to choroidal thinning [1]. In fact, a small but significant choroidal thinning was observed at the 6 D accommodation demand, which was greatest in the temporal and inferotemporal parafoveal choroid and increased with increasing eccentricity from the fovea. The regional variation in parafoveal thinning corresponds to the distribution of nonvascular smooth muscle within the uvea, which may implicate these cells as the potential mechanism by which the choroid thins during accommodation [4].

Another study by Breher et al. [25] evidenced changes in choroidal thickness, horizontal retinal radius of curvature, and the horizontal-vertical growth ratio, showing significant correlations with axial length and/or refractive error. Thus, retinal shape and choroidal thickness, but not foveal pit morphology, are altered by myopia-induced eye growth. Something similar was observed in the present study, with thinner peripheral retinas and changes in eccentricity after reading with both devices and different lighting conditions, due to the influence of accommodation rather than myopia.

Hoseini-Yazdi et al. [26] suggested that environmental light regulates ocular growth through mechanisms that may be mediated by melanopsin retinal ganglion cells (mRGCs). In their study, they aimed to examine the choroidal thickness changes following brief stimulation of melanopsin-expressing mRGC axons at the optic disc with blue light in a group of healthy emmetropic and myopic subjects. Sustained refractive error-dependent thickening of the choroid was observed, with brief optic disc stimulation with blue light. This choroidal response may be related to a short wavelength sensitive mRGC signaling pathway, given the lack of a choroidal response with red light stimulation.

On the other hand, the study by Li et al. [27] provides a quantitative reference for the impacts of the expansion in retinal contour on ocular aberrations. This is useful for the wide-angle eye modeling procedure, indicating that finer modeling of the retinal contour is required to achieve a more accurate prediction of peripheral defocus at the last step of the eye modeling procedure. In addition, this study offers new perspectives to investigate the optical mechanism of myopia progression, and the unique role of astigmatism in retinal growth has been discovered. This suggests that further longitudinal studies should be performed to follow peripheral aberrations and peripheral eye longitudes across the two-dimensional visual field in significant astigmatism. This represents a potential approach to uncovering optical features that can directly manipulate myopia progression or its activation with accommodation after long periods of reading.

Regarding retinal shape, a few studies have reported changes in the refractive power of the eye as a function of the light level conditions [28–30]. In that sense, night myopia is the modification (increase) in ocular refraction in low light conditions [31]. Prior to our work, retinal shape was described as a function of conical equations using magnetic resonance imaging. A study reported by Verkicharla et al. [32] concluded that, in myopia, the retinal shape tends to steepen at the posterior pole and flatten far from the pole. Then, if light conditions can induce the so-called night myopia phenomenon and retinal shape is sensitive to ocular refraction, it is consistent to ask if retinal morphological changes can occur while reading under variable light conditions. Since the luminance of the screens were somewhat different, especially at maximum lighting conditions, it was found that the higher the iPad light, the higher the retinal peripheral volume ($6.40 \pm 0.41 \text{ mm}^3$ high lighting volume vs. $6.32 \pm 0.44 \text{ mm}^3$ low lighting volume; $p = 0.023$), as was described in the results section and Figure 6, and no differences were found when reading with an Ebook, which was evaluated. Our developed retinal segmentation algorithm that was applied to OCT images acquired for the different reading and light level conditions described in Methods revealed lower eccentricity values at the peripheral locations than the central retina (i.e., tendency to a more parabolic shape at the periphery). At the central retina,

the computed eccentricity values were significantly lower in high-level conditions while reading with the iPad with regard to the basal values. At the periphery, both with iPad and Ebook devices showed significant changes in retinal shape in both high- and low-light conditions (see Figure 8).

Finally, when comparing the relative changes in eccentricity while reading a single electronic device as a function of the lighting level, significant changes were found for the Ebook device only (Figure 8). In both the central and peripheral retina, the eccentricity values were significantly lower under low light conditions. In addition, the retina significantly tended to change from a parabolic into a hyperbolic shape from the center to the retina.

5. Conclusions

In conclusion, the effect of illumination on retinal shape and thickness was demonstrated. Hence, it would be interesting to see whether variation of the central subfield or parafoveal retinal thickness may correlate more strongly with lighting conditions. Our findings indicate that young people can recover visual quality after five minutes of reading tasks at different lighting levels. The central retina quickly recovers both its shape and thickness, while peripheral retinal expansion remains altered after these near tasks, especially at low lighting levels.

Author Contributions: E.O.-H.: Conceptualization (equal); Investigation (equal); Methodology (equal); Data curation (equal); Resources (equal); Writing—review and editing (equal). F.J.Á.: Conceptualization (equal); Investigation (equal); Methodology (equal); Data curation (equal); Resources (equal); Software (equal); Writing—review and editing (equal). G.F.-E.: Data curation (lead); Writing—review and editing (equal). A.S.-C.: Conceptualization (equal); Investigation (equal); Methodology (equal); Data curation (equal); Resources (equal); Writing—review and editing (equal). All authors have read and agreed to the published version of the manuscript.

Funding: This research was funded by the Agencia Estatal de Investigación, Ministerio de Ciencia e Innovación of the Spanish Government (Grant PID2019-107058RB-I00 funded by MCIN/AEI/10.13039/501100011033), the European Union’s Horizon 2020 research and innovation programme under the Marie Skłodowska-Curie grant agreement No 956720, Gobierno de Aragón-Departamento de Ciencia, Universidad y Sociedad del Conocimiento-No LMP39_21, and Fundación Ibercaja and University of Zaragoza No JIUZ-2021-CIE-03.

Institutional Review Board Statement: The study was conducted in accordance with the Declaration of Helsinki and approved by the Comité de Ética de la Investigación de la Comunidad de Aragón (CEICA), with reference PI21-074.

Informed Consent Statement: Informed consent was obtained from all subjects involved in the study.

Data Availability Statement: The data sets of the current study are available from the corresponding author upon reasonable request.

Conflicts of Interest: The authors declare that they have no known competing financial interests or personal relationships that could have appeared to influence the work reported in this paper.

References

1. Logan, N.S.; Radhakrishnan, H.; Cruickshank, F.E.; Allen, P.M.; Bandela, P.K.; Davies, L.N.; Hasebe, S.; Khanal, S.; Schmid, K.L.; Vera-Diaz, F.A. IMI Accommodation and binocular vision in myopia development and progression. *Investig. Ophthalmol. Vis. Sci.* **2021**, *62*, 4. [[CrossRef](#)] [[PubMed](#)]
2. Read, S.A.; Fuss, J.A.; Vincent, S.J.; Collins, M.J.; Alonso-Caneiro, D. Choroidal changes in human myopia: Insights from optical coherence tomography imaging. *Clin. Exp. Optom.* **2019**, *102*, 270–285. [[CrossRef](#)] [[PubMed](#)]
3. Croft, M.A.; Peterson, J.; Smith, C.; Kiland, J.; Nork, T.M.; McDonald, J.P.; Katz, A.; Hetzel, S.; Lütjen-Drecoll, E.; Kaufman, P.L. Accommodative movements of the choroid in the optic nerve head region of human eyes, and their relationship to the lens. *Exp. Eye Res.* **2022**, *222*, 109124. [[CrossRef](#)] [[PubMed](#)]
4. Woodman-Pieterse, E.C.; Read, S.A.; Collins, M.J.; Alonso-Caneiro, D. Regional changes in choroidal thickness associated with accommodation. *Investig. Ophthalmol. Vis. Sci.* **2015**, *56*, 6414–6422. [[CrossRef](#)] [[PubMed](#)]

5. Woodman, E.C.; Read, S.A.; Collins, M.J. Axial length and choroidal thickness changes accompanying prolonged accommodation in myopes and emmetropes. *Vision Res.* **2012**, *72*, 34–41. [[CrossRef](#)] [[PubMed](#)]
6. Chui, T.Y.P.; Yap, M.K.H.; Chan, H.H.L.; Thibos, L.N. Retinal stretching limits peripheral visual acuity in myopia. *Vision Res.* **2005**, *45*, 593–605. [[CrossRef](#)]
7. Song, H.; Chui, T.Y.P.; Zhong, Z.; Elsner, A.E.; Burns, S.A. Variation of cone photoreceptor packing density with retinal eccentricity and age. *Investig. Ophthalmol. Vis. Sci.* **2011**, *52*, 7376–7384. [[CrossRef](#)]
8. Song, A.-P.; Wu, X.-Y.; Wang, J.-R.; Liu, W.; Sun, Y.; Yu, T. Measurement of retinal thickness in macular region of high myopic eyes using spectral domain OCT. *Int. J. Ophthalmol.* **2014**, *7*, 122.
9. Lam, D.S.C.; Leung, K.S.; Mohamed, S.; Chan, W.; Palanivelu, M.S.; Cheung, C.Y.L.; Li, E.Y.M.; Lai, R.Y.K.; Leung, C.K. Regional variations in the relationship between macular thickness measurements and myopia. *Investig. Ophthalmol. Vis. Sci.* **2007**, *48*, 376–382. [[CrossRef](#)]
10. Cheng, S.C.K.; Lam, C.S.Y.; Yap, M.K.H. Retinal thickness in myopic and non-myopic eyes. *Ophthalmic Physiol. Opt.* **2010**, *30*, 776–784. [[CrossRef](#)]
11. Hwang, Y.H.; Kim, Y.Y. Macular thickness and volume of myopic eyes measured using spectral-domain optical coherence tomography. *Clin. Exp. Optom.* **2012**, *95*, 492–498. [[CrossRef](#)] [[PubMed](#)]
12. Tan, C.S.H.; Cheong, K.X.; Lim, L.W.; Li, K.Z. Topographic variation of choroidal and retinal thicknesses at the macula in healthy adults. *Br. J. Ophthalmol.* **2014**, *98*, 339–344. [[CrossRef](#)] [[PubMed](#)]
13. Abbott, C.J.; Grünert, U.; Pianta, M.J.; McBrien, N.A. Retinal thinning in tree shrews with induced high myopia: Optical coherence tomography and histological assessment. *Vision Res.* **2011**, *51*, 376–385. [[CrossRef](#)] [[PubMed](#)]
14. Fulk, G.W.; Cyert, L.A.; Parker, D.A. Seasonal variation in myopia progression and ocular elongation. *Optom. Vis. Sci.* **2002**, *79*, 46–51. [[CrossRef](#)] [[PubMed](#)]
15. Donovan, L.; Sankaridurg, P.; Ho, A.; Chen, X.; Lin, Z.; Thomas, V.; Smith, E.L., III; Ge, J.; Holden, B. Myopia progression in Chinese children is slower in summer than in winter. *Optom. Vis. Sci. Off. Publ. Am. Acad. Optom.* **2012**, *89*, 1196. [[CrossRef](#)] [[PubMed](#)]
16. Cui, D.; Trier, K.; Ribel-Madsen, S.M. Effect of day length on eye growth, myopia progression, and change of corneal power in myopic children. *Ophthalmology* **2013**, *120*, 1074–1079. [[CrossRef](#)]
17. Gwiazda, J.; Deng, L.; Manny, R.; Norton, T.T. Seasonal variations in the progression of myopia in children enrolled in the correction of myopia evaluation trial. *Investig. Ophthalmol. Vis. Sci.* **2014**, *55*, 752–758. [[CrossRef](#)]
18. Read, S.A.; Collins, M.J.; Vincent, S.J. Light exposure and eye growth in childhood. *Investig. Ophthalmol. Vis. Sci.* **2015**, *56*, 6779–6787. [[CrossRef](#)]
19. McAlinden, C.; Khadka, J.; Pesudovs, K. Precision (repeatability and reproducibility) studies and sample-size calculation. *J. Cataract. Refract. Surg.* **2015**, *41*, 2598–2604. [[CrossRef](#)]
20. Armstrong, R.A. Statistical guidelines for the analysis of data obtained from one or both eyes. *Ophthalmic Physiol. Opt.* **2013**, *33*, 7–14. [[CrossRef](#)]
21. Grzybowski, A.; Kanclerz, P.; Tsubota, K.; Lanca, C.; Saw, S.M. A review on the epidemiology of myopia in school children worldwide. *BMC Ophthalmol.* **2020**, *20*, 27. [[CrossRef](#)] [[PubMed](#)]
22. Wong, C.W.; Tsai, A.; Jonas, J.B.; Ohno-Matsui, K.; Chen, J.; Ang, M.; Ting, D.S.W. Digital Screen Time during the COVID-19 Pandemic: Risk for a Further Myopia Boom? *Am. J. Ophthalmol.* **2021**, *223*, 333–337. [[CrossRef](#)] [[PubMed](#)]
23. Landis, E.G.; Park, H.N.; Chrenek, M.; He, L.; Sidhu, C.; Chakraborty, R.; Strickland, R.; Iuvone, P.M.; Pardue, M.T. Ambient light regulates retinal dopamine signaling and myopia susceptibility. *Investig. Ophthalmol. Vis. Sci.* **2021**, *62*, 28. [[CrossRef](#)] [[PubMed](#)]
24. Fan, S.; Sun, Y.; Dai, C.; Zheng, H.; Ren, Q.; Jiao, S.; Zhou, C. Accommodation-induced variations in retinal thickness measured by spectral domain optical coherence tomography. *J. Biomed. Opt.* **2014**, *19*, 096012. [[CrossRef](#)] [[PubMed](#)]
25. Breher, K.; Ohlendorf, A.; Wahl, S. Myopia induces meridional growth asymmetry of the retina: A pilot study using wide-field swept-source OCT. *Sci. Rep.* **2020**, *10*, 10886. [[CrossRef](#)]
26. Hoseini-Yazdi, H.; Read, S.; Collins, M.J.; Schilling, T.; Bahmani, H. Sustained increase in human choroidal thickness associated with brief stimulation of the optic disc with short-wavelength blue light. *Investig. Ophthalmol. Vis. Sci.* **2022**, *63*, 4322-A0027.
27. Li, Q.; Fang, F. Contribution of the retinal contour to the peripheral optics of human eye. *Vision Res.* **2022**, *198*, 108055. [[CrossRef](#)]
28. Wald, G.; Griffin, D.R. The change in refractive power of the human eye in dim and bright light. *J. Opt. Soc. Am.* **1947**, *37*, 321–336. [[CrossRef](#)]
29. Leibowitz, H.W.; Owens, D.A. Anomalous myopias and the intermediate dark focus of accommodation. *Science* **1975**, *189*, 646–648. [[CrossRef](#)]
30. Epstein, D.; Ingelstam, E.; Jansson, K.; Tengroth, B. Low-luminance myopia as measured with a laser optometer. *Acta Ophthalmol.* **1981**, *59*, 928–943. [[CrossRef](#)]
31. Lopez-Gil, N.; Peixoto-de-Matos, S.C.; Thibos, L.N.; González-Méijome, J.M. Shedding light on night myopia. *J. Vis.* **2012**, *12*, 4. [[CrossRef](#)] [[PubMed](#)]
32. Verkicharla, P.K.; Mathur, A.; Mallen, E.A.H.; Pope, J.M.; Atchison, D.A. Eye shape and retinal shape, and their relation to peripheral refraction. *Ophthalmic Physiol. Opt.* **2012**, *32*, 184–199. [[CrossRef](#)] [[PubMed](#)]